Shear-sliding behavior of masonry
Numerical micro-modeling of triplet tests

Ferretti, Francesca; Mazzotti, C.; Esposito, Rita; Rots, Jan

Publication date
2018

Document Version
Accepted author manuscript

Published in
Computational Modelling of Concrete Structures

Citation (APA)
Ferretti, F., Mazzotti, C., Esposito, R., & Rots, J. (2018). Shear-sliding behavior of masonry: Numerical micro-modeling of triplet tests. In G. Meschke, B. Pichler, & J. G. Rots (Eds.), *Computational Modelling of Concrete Structures: Proceedings of the Conference on Computational Modelling of Concrete and Concrete Structures* (pp. 941-952). CRC Press.

Shear-sliding behavior of masonry: numerical micro-modeling of triplet tests

F. Ferretti & C. Mazzotti
DICAM Department, University of Bologna, Italy

R. Esposito & J.G. Rots
Department of Structural Engineering, Delft University of Technology, The Netherlands

ABSTRACT: Masonry is a composite material, whose behavior is strongly influenced by the presence of vertical and horizontal mortar joints, weak elements along which the shear failure usually occurs. The scope of the present work was to investigate factors that could affect the shear-sliding behavior of masonry, by performing numerical simulations of triplet tests conducted on calcium silicate brick masonry specimens with two different bond patterns. In the numerical analyses, a simplified micro-modeling strategy was adopted. A composite interface model was used, including a tension cut-off, a Coulomb friction criterion and a compressive cap. The numerical models were validated through comparisons with results from experimental tests, in terms of failure load, post-peak behavior and specimen deformability. Moreover, factors that could influence the shear-sliding behavior of masonry were analyzed by performing parametric studies. The simplified-micro modeling confirmed to be a very efficient strategy to capture the nonlinear behavior of masonry.

1 INTRODUCTION

The shear failure modes of a masonry structural element – toe crushing associated to rocking, sliding or diagonal cracking – depend mainly on its geometry, boundary conditions, level of compression applied, quality of the component materials and texture (Magenes & Calvi 1997). Regarding brick masonry, the presence of horizontal and vertical mortar joints surely affects the shear response of a masonry pier. Indeed, in many cases, they represent planes of weakness along which the failure occurs (Lourenço 1996, Rots 1997). When dealing with the shear-sliding failure of masonry panels, according to the Coulomb friction criterion, the local properties of the interface between mortar and brick, in terms of initial shear strength and friction coefficient, are the most important parameters to be evaluated.

Experimental laboratory tests may be performed for the evaluation of the mortar joint shear strength. To ensure the reliability of the results in a compression-shear test, various aspects have to be taken into account (Riddington et al. 1997). First of all, normal and shear stress distributions should be uniform along the sliding mortar joint. Secondly, the failure should initiate far away from the joint edges and should propagate quickly on the entire length of the joint. Finally, the presence of tensile stresses should be checked and avoided since they could affect the test outcomes.

Due to the difficulty in finding a testing procedure satisfying all the aforementioned aspects, many different test methods have been proposed and studied in the past (Drysdale et al. 1979, Stöckl et al. 1990, Riddington & Jukes 1994, Van der Pluijm 1999). They basically differed one from another in the geometry of the specimen – e.g. considering one or more bed joints – and in the loading arrangement. Few test methods included the presence of head joints (Atkinson 1989). Finite element analyses were also carried out to investigate peculiar aspects of the different methodologies, highlight their advantages and disadvantages and propose new test methods (Jukes & Riddington 2000, Popal & Lissel 2010, Montazerolghaem & Jaeger 2014).

A particular focus is here devoted to the triplet test, as proposed by the standard EN 1052-3 (Fig. 1). During the test, the specimen is subjected to a constant lateral pre-compression, while a shear load is applied to the central brick to produce its sliding. It was introduced since its execution does not need special or complex equipment (if compared to other testing methods), and, above all, it was found to be adequate to provide reliable results (Vermeltfoort, 2010). However, the main issues of this test are: (i) stress concentrations close to the loading points; (ii) presence of bending moment along the joint, which causes non-uniform stress distributions and can lead to undesired failure, especially for very low value of pre-compression. To partially overcome these problems, the position of the support in the standard set-

up ensure the minimum bending moment present in the joint (Jukes & Riddington 2001). By performing the triplet test using a displacement controlled procedure, all properties characterizing the shear-sliding behavior of mortar joints, according to a Coulomb friction model, can be derived: shear strength, cohesion and friction softening, mode-II fracture energy, dilatancy.

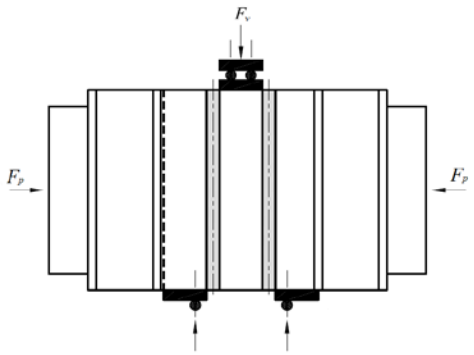

Figure 1. Triplet test setup, EN1052-3.

The scope of the present work was to investigate factors that could affect the shear-sliding behavior of masonry. In particular, the influence of the boundary conditions and the role of dilatancy were studied in detail. Attention was also paid to the development of the stress distributions along the mortar joints and the cracking formation and evolution. To these purposes, numerical simulations of triplet tests conducted on calcium silicate brick masonry were performed. The mechanical parameters to be used in the numerical models were obtained from experimental tests on standard triplet specimens. Comparisons between numerical and experimental results were carried out to validate the numerical model, which was also applied to the case of a modified triplet test geometry, as will be explained in the following sections.

2 TRIPLET TEST

In the triplet test (EN 1052-3), a sliding failure is reproduced, in which the mortar joint is subjected to a constant level of orthogonal compression and to an increasing tangential shear load.

With the objective of investigating the shear properties of bed joints in calcium silicate brick masonry, a laboratory experimental campaign was carried out at Delft University of Technology on replicated masonry samples (Jafari & Esposito 2016). The triplet test setup is presented in Figure 2. Specimens were built using calcium silicate bricks (dimensions: 214x102x72 mm^3) and cementitious mortar (joint thickness: 10 mm). At the beginning of the test, the pre-compression was applied by means of a manually operated hydraulic jack (load controlled) and kept constant. The lateral steel plates ensured the diffusion of the compressive load on the entire lateral surfaces of the sample. The shear load was then applied in the vertical direction, on the middle brick, using a displacement controlled apparatus with a 100 kN hydraulic jack and a spherical joint. The shear displacement rate was equal to 0.005 mm/s during the loading phase and to 0.05 mm/s in the unloading phase. During the test, displacements tangential and orthogonal to the mortar joints were continuously measured with Linear Variable Differential Transformers (LVDT), positioned on both sides of the specimen. Nine specimens were tested at three levels of pre-compression: 0.20 N/mm^2, 0.60 N/mm^2 and 1.20 N/mm^2. Moreover, one sample was tested with a pre-compression equal to 0.05 N/mm^2 to better estimate the initial shear strength.

Figure 2. Triplet test experimental setup.

The typical load-displacement relationship was characterized by an initial almost linear behavior up to the peak load, followed by a softening branch and a residual tail, corresponding to a dry friction condition.

By performing the test with different levels of pre-compression, and plotting the peak shear strength τ against the normal compressive stress σ, it was possible to calibrate the Coulomb friction failure criterion:

$$\tau = c_0 + \sigma \tan \phi_0 , \quad (1)$$

where c_0 is the cohesion or initial shear strength, and ϕ_0 is the friction angle. In an analogous way, by plotting the residual shear strength τ_{res} against the normal compressive stress σ and performing a linear interpolation, the residual failure criterion could be evaluated as well, which was characterized by a residual shear strength c_{res} and a residual friction ϕ_{res}.

The mode-II fracture energy G_f^{II} was calculated for each test and its linear dependence on the pre-compression level can be described with the following equation (Rots 1997, Van der Pluijm 2000):

$$G_f^{II} = a\sigma + b , \quad (2)$$

where *a* and *b* were determined from linear regression of experimental data.

Uplift upon shearing was observed during experimental tests. Therefore, parameters governing the dilatant behavior of mortar joints were evaluated by least-squares fitting of experimental data, according to the variable formulation for dilatancy (Van Zijl 2004):

$$\tan\psi = \tan\psi_0 \left\langle 1 - \frac{\sigma}{\sigma_u} \right\rangle e^{-\delta v_p}, \quad (3)$$

where v_p is the plastic shear displacement, ψ_0 is the dilatancy angle at zero confining stress and shear slip, σ_u is the pre-compression level at which the dilatancy goes to zero, and δ is the dilatancy shear-slip degradation coefficient. It has been found in previous researches (Van der Pluijm 2000, Van Zijl 2004) that, during the sliding failure, the uplift is arrested at high pre-compression and large plastic shear displacement.

The determined mechanical properties are reported in Table 1 and were used as input parameters for the numerical simulations. The Young's moduli and Poisson's ratios for bricks and mortar were determined through uniaxial compression tests on the single components and on masonry wallets.

The standard triplet specimen, according to the European Standard (EN 1052-3), is composed by three bricks, arranged with a stacked bond pattern (Fig. 3a). However, considering a typical masonry pattern, the situation in which two bricks slide one over the other is not common. A more representative condition is the one in which also head joints are included. In order to study the influence of the vertical mortar joints on the sliding failure of masonry, modified triplet specimens were tested, characterized by a running bond pattern (Fig. 3b).

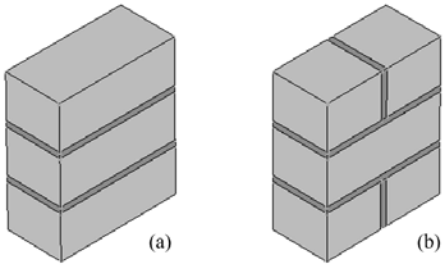

Figure 3. Specimen geometry: (a) standard triplet specimen (stacked bond); (b) modified triplet specimen (running bond).

3 SIMPLIFIED MICRO-MECHANICAL MODELING

Several modeling strategies can be used for masonry, depending on the way in which the constituents (units and mortar) and their interactions are considered. In general, it is possible to distinguish between a micro-modeling strategy, in which the single components are individually taken into account, or a macro-modeling strategy, in which masonry is modeled as a composite (Lourenco et al. 1995, Rots 1997). In the numerical analyses here presented, a micro-mechanical model was chosen, given the high level of accuracy needed to study the sliding failure along the mortar joint and considering the small dimensions of the samples.

In the framework of micro-modeling, it is also possible to distinguish between detailed and simplified strategies, as classified in previous researches (Lourenço et al. 1995, Rots 1997). Differently from the detailed strategy, which implies the use of continuum elements for both units and mortar joints and of interface elements for adhesion surfaces (Fig. 4a), in the simplified micro-modeling, the mortar joints are modeled as zero-thickness interface elements and the units are modeled using continuum elements with expanded geometry, so to maintain the overall dimensions of the sample unchanged (Fig. 4b). The simplified micro-modeling strategy was considered adequate to capture the shear behavior observed in the tests, also allowing to reduce the computational effort, and was adopted in this research.

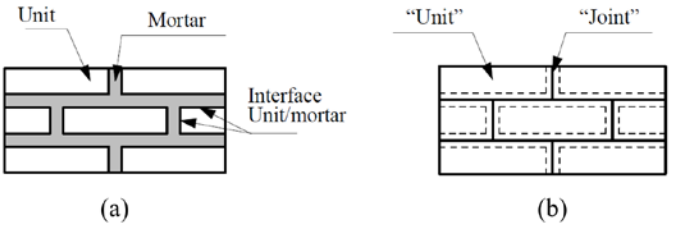

Figure 4. Modeling strategies for masonry structures: (a) detailed micro-modeling; (b) simplified micro-modeling. (Lourenco 1996).

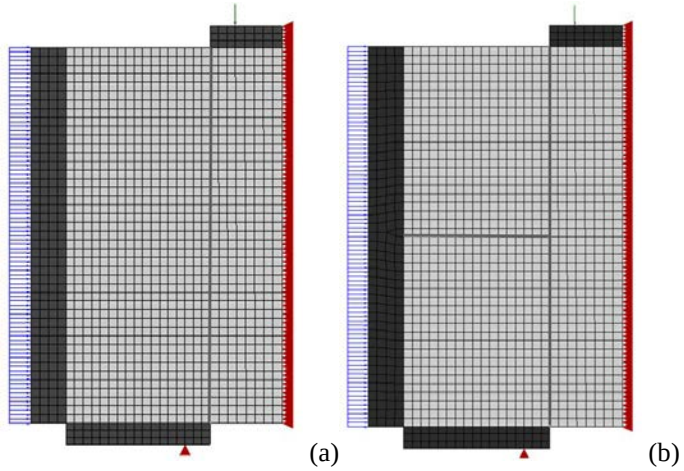

Figure 5. Finite element model: (a) standard triplet specimen; (b) modified triplet specimen.

The details of the mesh used in the numerical models are shown in Figure 5 for the different triplet

specimen typologies. 2D models were adopted and, making use of symmetry, only half of the sample was considered. According to the simplified micro-modeling approach, bricks were modeled using quadratic 8-noded plane stress elements, while line 3-noded interface elements were adopted to model the zero-thickness mortar joints.

A linear elastic behavior was considered for plane stress elements, with the typical stress-strain relations for continuum elements. For interface elements, the constitutive behavior can be described through a relationship between the stresses and the relative displacements along the interface, which in the linear elastic range reads:

$$\begin{bmatrix} \sigma \\ \tau \end{bmatrix} = \begin{bmatrix} k_n & 0 \\ 0 & k_t \end{bmatrix} \cdot \begin{bmatrix} \Delta u \\ \Delta v \end{bmatrix}, \quad (4)$$

where σ and τ are the compressive and shear stresses along the interface, k_n and k_t are the normal stiffness and the shear stiffness, respectively, and Δu and Δv are the normal and tangential relative displacements.
In the simplified micro-modeling, the elastic stiffness parameters of the brick-mortar interfaces were evaluated considering the actual dimensions of units and mortar joints and their mechanical properties (Rots 1997):

$$k_n = \frac{E_b E_m}{t_m \left(E_b - E_m\right)} \quad (5)$$

$$k_t = \frac{G_b G_m}{t_m \left(G_b - G_m\right)} = \frac{E_b E_m}{2t_m \left(E_b \left(1+\nu_m\right) - E_m \left(1+\nu_b\right)\right)}, \quad (6)$$

where E_b and G_b are the elastic and shear modulus of the bricks, E_m and G_m are the elastic and shear modulus of the mortar, and t_m is the mortar joint thickness.

Since the sliding failure was expected to take place along the bed joint, the nonlinear behavior was only assigned to this failure plane. A composite interface model was used, including a tension cut-off, a Coulomb friction criterion and a compressive cap (Fig. 6).

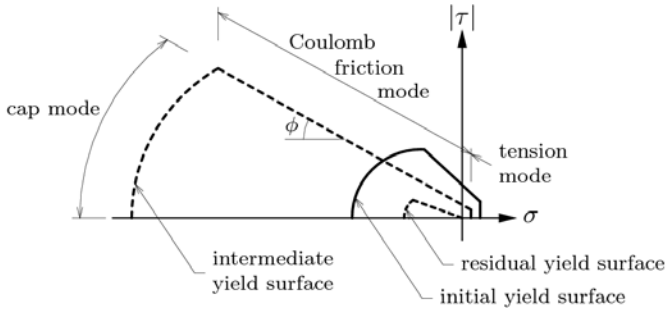

Figure 6. Composite interface model for nonlinear interface elements.

Exponential softening for both tension and shear failure (mode-I and mode-II failure types, respectively) was included, while a hardening/softening behavior was introduced for compression. The complete description of the numerical implementation is not reported here, but the reader can refer to Lourenco (1996).

With reference to the Coulomb friction model, which describes the shear-sliding behavior observed in experimental tests, the yielding function reads:

$$f\left(\sigma, \kappa_2\right) = |\tau| + \sigma \tan\phi(\kappa_2) - c(\kappa_2). \quad (7)$$

The cohesion and friction softening are defined according to the following expressions:

$$c(\kappa_2) = c_0 \cdot \exp\left(-\frac{c_0}{G_f^{II}} \kappa_2\right) \quad (8)$$

$$\tan\phi(\kappa_2) = \tan\phi_0 + (\tan\phi_{res} - \tan\phi_0) \frac{c_0 - c(\kappa_2)}{c_0}. \quad (9)$$

In the previous equations, c_0 is the cohesion of the brick-mortar interface, ϕ_0 and ϕ_{res} are the initial and the residual friction angle, respectively, G_f^{II} is the mode-II fracture energy, and κ_2 is a scalar indicating the amount of softening, assumed equal to the plastic shear displacement.
A non-associated plastic potential is considered:

$$g_2 = |\tau| + \sigma \tan\psi - c_0 \quad (9)$$

with a variable dilatancy angle ψ, depending on the normal stress and the plastic shear displacement, according to Equation 3.

The input parameters used in the numerical models for masonry are reported in Table 1, where distinction is made between parameters obtained directly from tests and calibrated ones. Concerning calibrated parameters, tensile strength and mode-I fracture energy were determined as a fraction of the cohesion and mode-II fracture energy, respectively (Rots 1997). The parameters for the Coulomb friction model were calibrated from standard triplet tests results, as explained in Section 2, and then used also in the numerical simulations for modified triplets.

To entirely reproduce the test setup, the loading steel plates were also modeled using quadratic plane stress elements, with a linear elastic behavior. The elastic modulus E_s and the Poisson's ratio ν_s for steel were equal to 210000 N/mm^2 and 0.30, respectively. Interface elements were adopted for the brick-to-steel contact planes. These elements were modeled as a no-tension material, with a dummy value for the normal stiffness in compression, to allow both the transfer of compressive stress and the separation between steel plates and bricks in presence of tensile stresses. A very low value (10 N/mm^3) was given to

the shear stiffness to avoid lateral confinement of bricks.

Numerical simulations were performed with the finite element software DIANA FEA (Release 10.1), at 4 different pre-compression levels σ_p (0.05 – 0.20 – 0.60 – 1.20 N/mm^2) to reproduce the loading conditions of the experimental tests. The shear load was applied as an increasing displacement on the top plate. Regular Newton-Raphson method was adopted to solve the nonlinear problem.

Table 1. Input parameters for masonry.

	Description	Symbol	Units	Value
Parameters from tests	Elastic modulus of brick	E_b	[N/mm^2]	10000
	Poisson's ratio of brick	ν_b	-	0.16
	Elastic modulus of mortar	E_m	[N/mm^2]	1088
	Poisson's ratio of mortar	ν_m	-	0.20
	Cohesion	c_0	[N/mm^2]	0.13
	Friction angle	ϕ_0	[rad]	0.463
	Residual friction angle	ϕ_{res}	[rad]	0.463
	Compressive strength	f_c	[N/mm^2]	6.35
	Compr. fracture energy	G_f^c	[N/mm]	20
	Equiv. plastic shear displ.	κ_p	-	0.005
Calibrated Parameters	Interface normal stiffness	k_n	[N/mm^3]	122.1
	Interface shear stiffness	k_t	[N/mm^3]	50.7
	Tensile strength	f_t	[N/mm^2]	0.09
	Mode-I fracture energy	G_f^I	[N/mm]	0.01
	Dilatancy angle	ψ_0	[rad]	0.374
	Confining normal stress	σ_u	[N/mm^2]	0.58
	Exp. degradation coeff.	δ	-	9.63
	Mode-II fracture energy	a	[mm]	0.114
	($G_f^{II} = a\sigma + b$)	b	[N/mm]	0.011

4 NUMERICAL RESULTS

In this section, results of the numerical simulations are presented for standard and modified triplet tests, and compared with experimental results. To properly describe the sliding failure through the Coulomb friction domain, experimental results obtained from standard triplet tests were used to calibrate the model.

4.1 *Standard triplet test*

The results of the numerical simulations for standard triplet tests, at each pre-compression level, are reported in Figure 7 and Figure 8 in terms of shear stress τ vs. tangential displacement δ_v and normal displacement δ_u vs. tangential displacement δ_v, respectively. They are compared with experimental results. Concerning τ-δ_v diagram, it can be noticed how numerical results are in good agreement with the experimental ones, for all pre-compression levels. The presence of multiple peaks in some of the experimental curves could indicate that the failure was not activated at the same time on both mortar joints. However, given the symmetric model considered, this aspect is not studied here. Looking at Figure 8, it can be noticed that, for pre-compression levels of 0.60 N/mm^2 and 1.20 N/mm^2, the experimental curves show a compression orthogonal to the bed joint, which is not well captured by the numerical results. This can be explained by some setup features – e.g. lateral loading plate not free to displace at high pre-compression stress levels – or by considering that the failure mode observed in these experimental tests, especially for the pre-compression level of 1.20 N/mm^2, was not a pure sliding failure along the brick-mortar interface but involved the mortar itself. Indeed, cracking in the mortar occurred along the compression lines, especially close to the upper joint edge. In order to capture the very low – even negative – values of normal displacements δ_u, variations to the numerical model could be made. On the one hand, a modification of the boundary conditions could be considered, as will be discussed in detail in Section 5.1. On the other hand, to properly describe the mortar failure, a detailed micro-modeling strategy, not reported in this work, could be adopted.

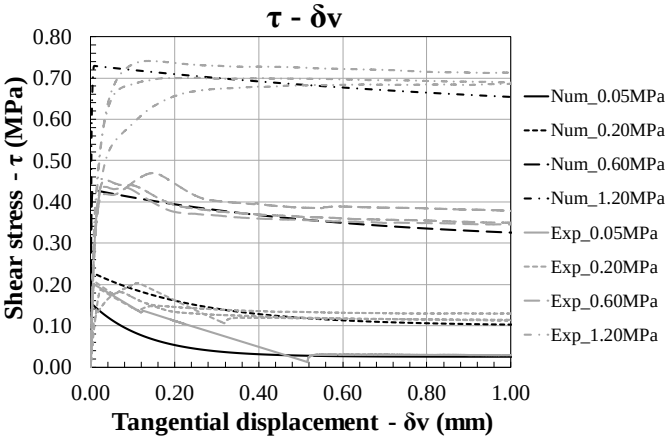

Figure 7. Standard triplet test, shear stress vs. tangential displacement.

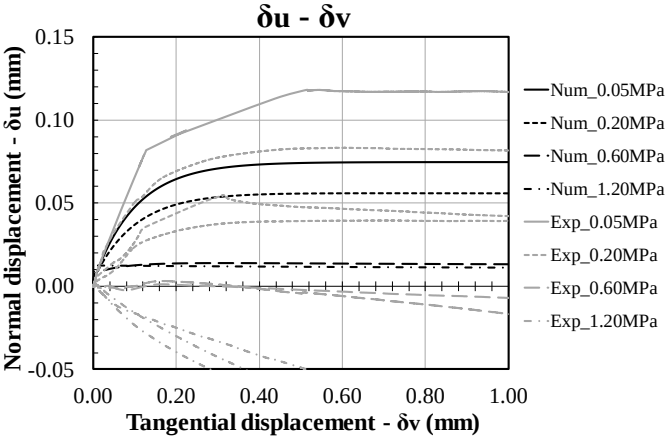

Figure 8. Standard triplet test, normal displacement vs. tangential displacement.

The principal stress distributions in Figure 9, reported as an example for a pre-compression level of 0.20 N/mm^2, show high stress concentrations close to the loading plates and the presence of a compressed strut.

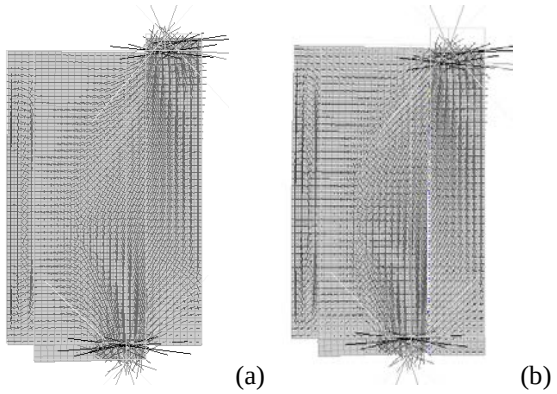

Figure 9. Standard triplet test at pre-compression 0.20 N/mm^2 – Principal stress distributions: (a) pre-peak (δ_v = 0.02 mm); (b) post-peak (δ_v = 0.08 mm).

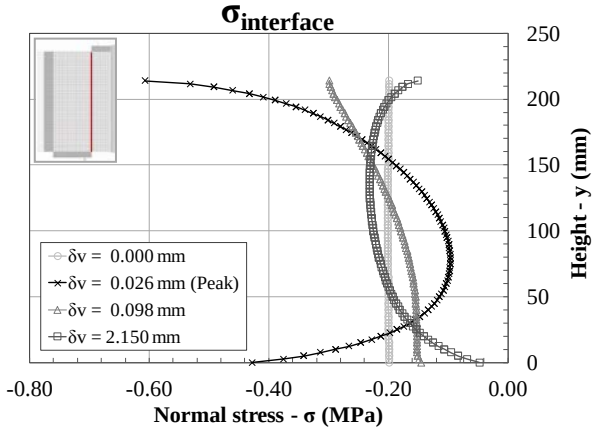

Figure 10. Standard triplet test at pre-compression 0.20 N/mm^2, normal stress evolution along the nonlinear interface.

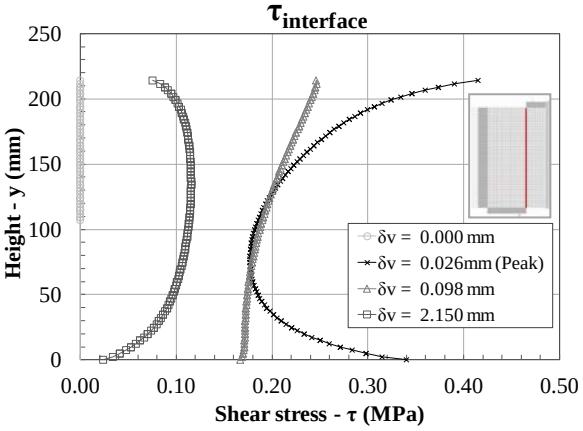

Figure 11. Standard triplet test at pre-compression 0.20 N/mm^2, tangential stress evolution along the nonlinear interface.

Considering the results of the nonlinear analyses for standard triplet specimens, it is interesting to investigate the development of the stress distributions along the joint and the propagation of the failure, given that they could influence the reliability of the results, as mentioned at the beginning.

In Figure 10 and Figure 11 the stress evolution along the sliding failure plane is shown, both for normal and tangential stresses, at pre-compression equal to 0.20 N/mm^2. It can be noticed that the stress distributions are not uniform along the joint and that concentrations of stresses occur at the joint edges, as already observed. Due to the diffusion of the shear load, in the first part of test, the normal compression increases at the joint extremities (always greater at the top), while it decreases in the middle of the specimen. In the post-peak phase, instead, the normal compression is greater at mid-height than at the extremities. The shear stress distributions develop accordingly.

Failure did not initiate far away from the joint edges but close to the bottom extremity and then propagated upwards. Nevertheless, a shear displacement increase of less than 0.01 mm was needed for it to propagate along the entire joint length.

Similar results were obtained in previous researches, where finite element analyses of different shear tests were performed and stress distributions compared (Riddington et al. 1997, Stöckl et al. 1990). In almost all shear tests, except the one proposed by Van der Pluijm (1999), non-uniform stress distributions were observed and peak stresses at the joint extremities were quite high.

4.2 *Modified triplet test*

The results of the numerical simulations for modified triplet tests are reported in terms of shear stress τ vs. tangential displacement δ_v (Fig. 12) and in terms of normal displacement δ_u vs. tangential displacement δ_v (Fig. 13). Experimental results are also included. It can be noticed a good agreement between numerical and experimental results, especially in the τ-δ_v diagram. In the δ_u-δ_v diagram, their agreement is quite good for almost all pre-compression levels, especially in correspondence of low tangential displacement values. Exceptions are represented by the sample tested at 0.05 N/mm^2 and by one specimen at 0.20 N/mm^2, which showed a great uplift upon shearing. The issue previously highlighted for standard triplets – which registered negative δ_u values for high pre-compression stresses – is here present only for two samples at pre-compression equal to 1.20 N/mm^2.

The results of the numerical analysis for modified triplet specimens are satisfactory if compared with experimental results, even if the numerical model was calibrated with results from standard triplet tests. This fact could be explained considering the failure modes observed in modified triplet tests. Indeed, in the majority of the cases, the sliding failure involved the brick-mortar interface close to the central brick. Only in few cases, the mortar continuity

between the head and bed joint was damaged. Therefore, the presence of the head joint, for the masonry typology investigated, did not seem to have a great influence on the outcomes of the tests, especially in terms of peak and residual shear loads.

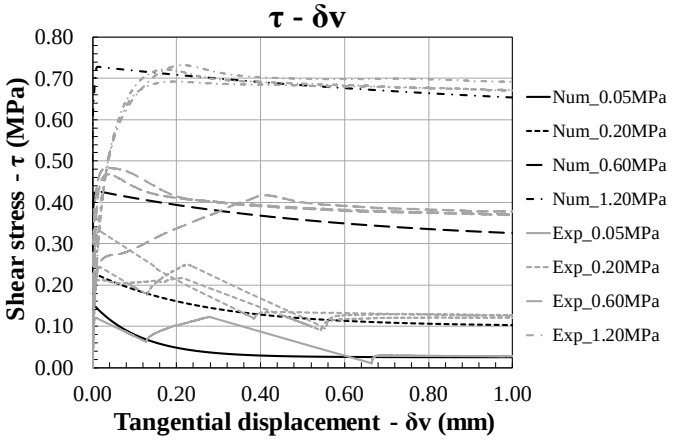

Figure 12. Modified triplet test, shear stress vs. tangential displacement.

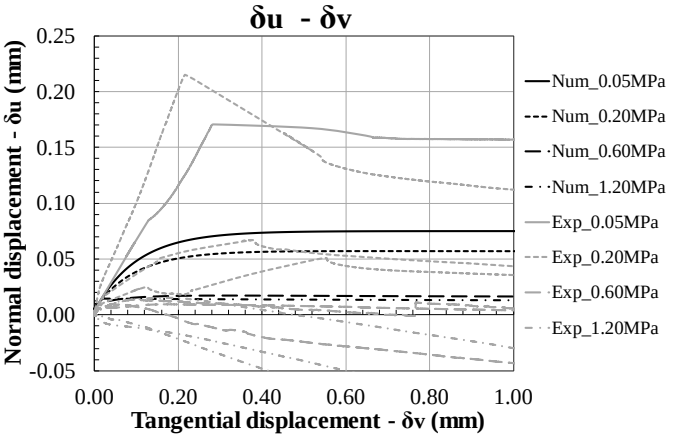

Figure 13. Modified triplet test, normal displacement vs. tangential displacement.

In Figure 14 and Figure 15 the stress evolution along the sliding failure plane is shown, both for normal and tangential stresses, at a pre-compression of 0.20 N/mm^2. As already observed for standard triplet tests, the stress distributions are not uniform along the joint and concentrations of normal stresses are present at the joint extremities. The jump in the stress distributions in correspondence of the head joint can be explained considering that the upper left brick was subjected to a deformation and a clockwise rotation. With respect to the standard triplet test distributions (Figs 10, 11), these movements caused, along the upper portion of the sliding surface, higher peak stresses at the top and reduced stresses in the middle, even leading to tensile stresses in a small portion of the sliding interface.

The normal stress evolution on the head joint is presented in Figure 16. Maximum values of compressive stresses are present at the right-end side, close to the sliding failure plane. This is consistent with the diffusion of the shear load inside the specimen and with the clockwise rotation of the upper left brick. With the failure propagation, the reduction of the compressive stresses along the head joint can be related to the reduction of the upper left brick deformation due to the lateral relaxation of the sample in the softening phase.

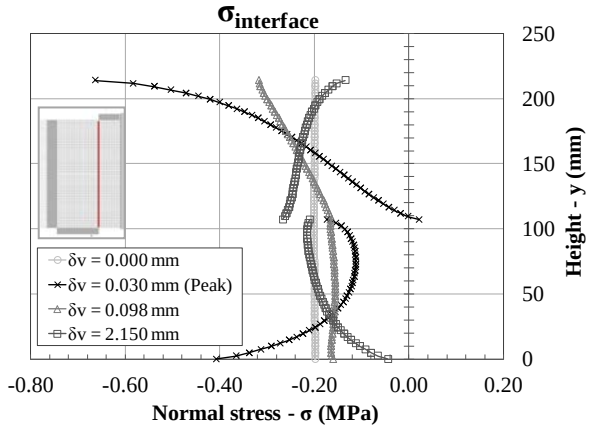

Figure 14. Modified triplet test at pre-compression 0.20 N/mm^2, normal stress evolution along the nonlinear interface.

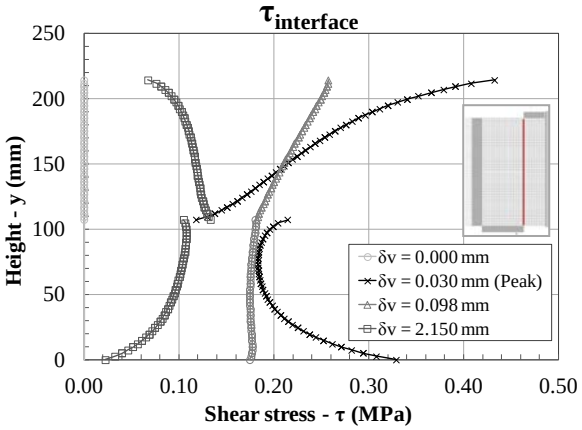

Figure 15. Modified triplet test at pre-compression 0.20 N/mm^2, tangential stress evolution along the nonlinear interface.

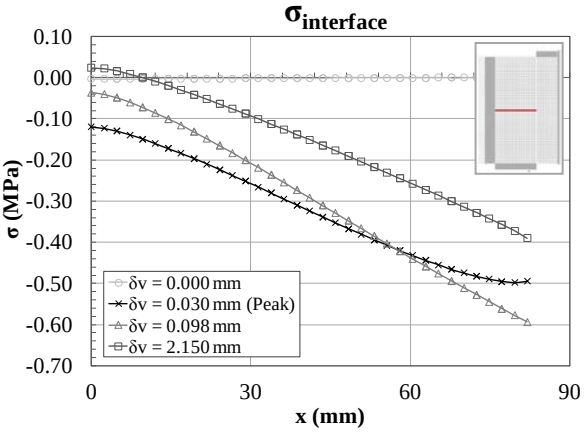

Figure 16. Modified triplet test at pre-compression 0.20 N/mm^2, normal stress evolution along the head joint.

5 PARAMETRIC STUDIES

In this section, some modifications to the numerical models are introduced with the aim of studying the influence of different parameters and testing conditions on the shear-sliding behavior of calcium silicate masonry.

5.1 *Influence of boundary conditions (standard triplet test)*

Dilatancy is one of the most important parameters governing the sliding failure of mortar joints. Indeed, the dilatant behavior of masonry could affect the results in two different ways, depending on the boundary conditions of the triplet tests. It could either produce an increase in the peak load, in case of restrained lateral displacement, or an increase in the displacements orthogonal to the bed joint, if the specimen is free to displace laterally. In particular, an increase in the shear capacity is determined by the fact that, during the sliding, when the uplift is restrained, the pre-compression level on the joint increases, which consequently leads to higher peak loads. Therefore, the way in which the pre-compression is applied to the sample plays a crucial role in the outcomes of the test.

To study the influence of the boundary conditions, additional numerical simulations were performed, in which the pre-compression load was applied as a constant lateral displacement, i.e. to reproduce the restrained displacements condition. The mechanical properties and the pre-compression levels considered were the same of the previous analyses. The results of the numerical simulations for laterally restrained model are here reported for standard triplet tests only.

The shear stress τ vs. tangential displacement δ_v diagrams are reported in Figure 17. It can be stated that the laterally restrained condition is not representative of standard triplet tests at low pre-compression stress levels, i.e. 0.05 N/mm^2 and 0.20 N/mm^2. Indeed, differently to what can be observed in Figure 7, the numerical curves do not correspond at all to the experimental ones. For higher pre-compression levels (0.60 N/mm^2 and 1.20 N/mm^2), instead, there is still a good agreement between numerical and experimental results. This is related to the fact that, in these latter cases, dilatancy is playing a very marginal role, given the high compression acting on the joint.

The normal displacement δ_u vs. tangential displacement δ_v diagrams are reported in Figure 18 for triplet tests at 0.60 N/mm^2 and 1.20 N/mm^2. Here, the results already presented for standard triplets with free lateral displacements are reported as well. By considering a restrained displacement condition, a better correspondence is found, especially at 0.60 N/mm^2 and for very low values of tangential displacements (< 0.20 mm). This is the most interesting portion of the diagram, corresponding to the activation of the sliding failure and the reaching of the peak load.

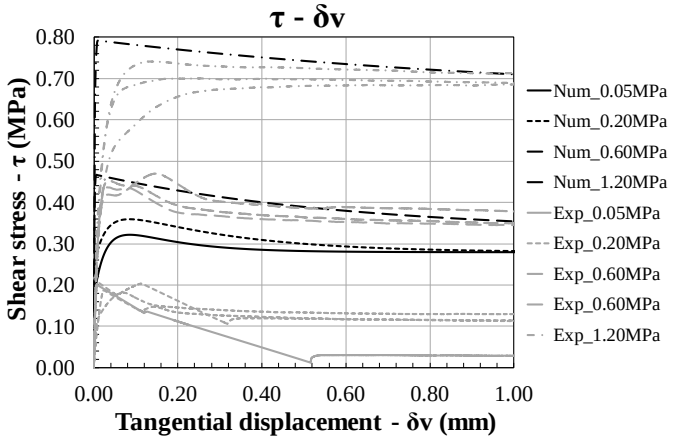

Figure 17. Standard triplet test with restrained lateral displacement, shear stress vs. tangential displacement.

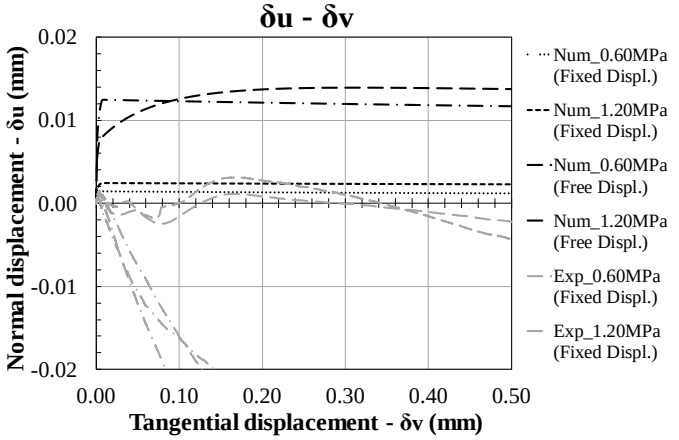

Figure 18. Standard triplet test, shear stress vs. tangential displacement – Free vs. restrained lateral displacement conditions.

5.2 *Influence of dilatancy parameters (modified triplets test)*

The uplift upon shearing is governed by the dilatancy function (Eq. 3) and, therefore, by the parameters ψ_0, σ_u and δ. In this context, parametric studies were performed for models with free lateral displacements, varying the values of these parameters. In the followings, results of numerical simulations for modified triplet tests are shown, where increased values of ψ_0 and σ_u were considered (Tab. 2). Indeed, experimental results showed that modified triplet specimens were characterized by higher normal displacements δ_u with respect to standard triplets. Given the observations reported in Section 5.1, the results were not expected to be different from the previous models in terms of shear capacity, but in terms of normal displacements. Figure 19 shows an increase in the normal uplift for all tests, except for the case with pre-compression equal to 1.20 N/mm^2.

Comparing it with Figure 13, it is possible to observe that a better agreement between numerical and experimental results is found, especially at low pre-compression levels.

Table 2. Modified dilatancy parameters.

Parameter	Symbol	Value
Dilatancy angle	ψ_0 [rad]	0.561 (+50%)
Confining normal stress	σ_u [N/mm^2]	0.70 (+20%)
Exp. degradation coeff.	δ	9.63

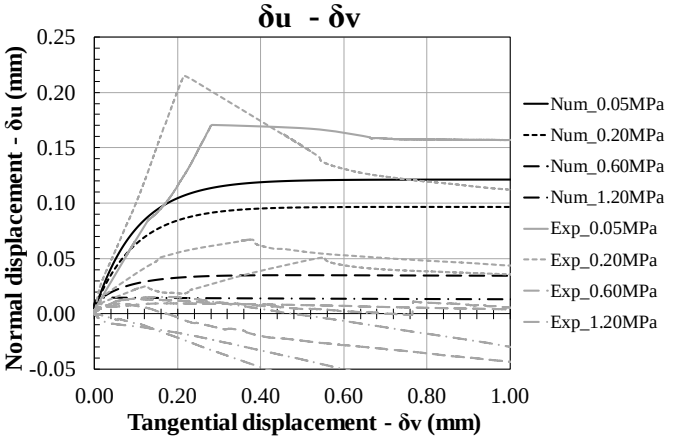

Figure 19. Modified triplet test, normal displacement vs. tangential displacement.

5.3 *Influence of the elastic properties of head joint (modified triplets test)*

With reference to the modified triplet specimens, parametric studies were carried out on the elastic stiffnesses of the head joint. Indeed, in the engineering practice, it is quite common to deal with masonry structures in which head joints have lower mechanical properties than bed joints. This is due to construction reasons and, moreover, to the fact that head joints are not subjected to compression during the curing. Therefore, imperfections or microcracks are often present. To simulate this situation, the elastic modulus of mortar was reduced by 50% and the elastic stiffness parameters of the interface elements were modified accordingly. Results are here reported in terms of normal stresses for the pre-compression level of 0.20 N/mm^2 (Fig. 20). Distributions at peak load and in the residual phase are shown and results from Figure 16 are also included. In presence of weak head joint, a 20% compressive stress reduction can be observed on the right-end side of the joint, in correspondence of the peak load (δ_v = 0.030 mm), as expected. In the residual phase, instead, where the shear load has already been transferred and a pure friction behavior can be observed, the two stress distributions almost coincide.

Differences were not observed neither in terms of peak and residual shear load nor in terms of orthogonal displacements. Similar observations can be done for the other pre-compression levels, which are not reported here, for sake of brevity.

The variation of the elastic properties of the head joint was not sufficient to influence the sliding failure during the triplet test. In order to consider different behaviors, e.g the failure within the head joint or in the contact point between head and bed joint, the use of a detailed micro-modeling strategy could be useful, in which nonlinearities could be assigned to the head joint. However, these variations were not considered here, given that the head joint was not involved in the sliding failure during experimental tests.

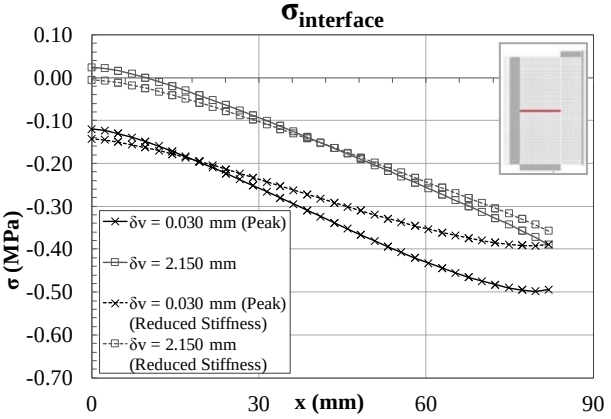

Figure 20. Modified triplet test at pre-compression 0.20 N/mm^2, normal stress evolution – Intact vs. weak head joint.

6 CONCLUSIONS

The numerical simulations of triplet tests presented in this paper were carried out to study the shear-sliding behavior of calcium silicate brick masonry. Two different geometries were considered: the standard triplet specimen and the modified one, characterized by a running bond pattern. A simplified micro-modeling strategy was adopted. The models were calibrated with results of standard triplet tests and then validated through comparisons between numerical and experimental results.

The obtained numerical results allowed to highlight which aspects could most affect the outcomes of the triplet tests. In particular, the influence of dilatancy and the boundary conditions were analyzed.

The influence of dilatancy on the results of the triplet test is strongly associated to the boundary conditions of the test itself. On the one hand, in case of restrained lateral displacements, an overestimation of the shear capacity was observed for samples at pre-compression equal to 0.05 N/mm^2 and 0.20 N/mm^2. At higher pre-compression levels, instead, the restrained displacements condition could partially capture the very low values registered for normal displacements. On the other hand, in case of free lat-

eral displacements, the dilatancy can affect the values of the normal displacements along the sliding failure plane. To investigate this aspect, parametric studies were performed on the variables defining the dilatancy function. In particular, for modified triplet tests, in which the registered uplift upon shearing was higher than in standard triplet tests, these parametric studies allowed to better capture the behavior of the samples, at least for low pre-compression levels.

The presence of a head joint did not have a great influence on the tests outcomes. This was confirmed both by numerical and experimental results and can be related to the specific masonry typology investigated. Indeed, the head joint was almost never involved in the failure process. Parametric studies were performed, reducing the normal and shear stiffness values, and the only difference in the results was represented by a change in the stress distributions along the head joint. In order to include failure modes involving the head joint, it is advisable to use a detailed micro-modeling strategy.

Aspects related to the triplet test setup and execution were analyzed and briefly discussed, such as the presence of non-uniform stress distributions along the sliding bed joint, the concentration of stresses at its extremities, the failure initiation and propagation. Even if the objective of the research was not to reduce or eliminate the influence that these aspects have on the test outcomes, they all represents intrinsic issues in the triplet test, which is important to be aware of.

In conclusion, the numerical simulations here presented allowed to gain a better understanding of the sliding failure in triplet tests. Future works can be done with the objective of better capturing the shear failure within the mortar at high pre-compression level. The detailed micro-modeling approach could be used with this purpose, in which failure inside the mortar can be included.

ACKNOWLEDGMENTS

The experimental tests used in this paper were performed at Delft University of Technology within the "Testing program 2016 for Structural Upgrading of URM Structures" financed by Nederlandse Aardolie Maatschappij (NAM) under contract number UI63654. The first author would like to acknowledge the "Marco Polo" mobility program of the University of Bologna, that provided funding for her visiting period at Delft University of Technology.

REFERENCES

Atkinson, R.H., Amadei, B., Saeb, S. & Sture, S. 1989. Response of masonry bed joints in direct shear. *Journal of Structural Engineering*, 115(9):2276-2296.

Drysdale, R.G., Vanderkeyl, R. & Hamid, A.A. 1979. Shear strength of brick masonry joints. *Proc. 5th Int. Brick and Block Mas. Conf., Washington D.C., 5-10 October 1979*.

EN 1052-3:2002. Method of test masonry – Part 3: Determination of initial shear strength. *European Standards (EN).*

Jafari, S. & Esposito, R. 2016. Material tests for the characterisation of replicated calcium silicate brick masonry. *Delft University of Technology, Report number C31B67WP1-9, 14 November 2016.*

Jukes, P. & Riddington, J.R. 2000. Finite element prediction of block triplet shear strength. *Proc. 12th Int. Brick and Block Mas. Conf., Madrid, 25-28 June 2000.*

Jukes, P. & Riddington, J.R. 2001. The failure of brick triplet test specimens. *Masonry International*, 15(1).

Lourenco, P.B., Rots, J.G. & Blaauwendraad, J. 1995. Two approaches for the analysis of masonry structures: micro and macro-modeling. *Heron*, 40(4):313-340.

Lourenco, P.B. 1996. Computational strategies for masonry structures, PhD thesis, Delft University of Technology.

Magenes, G. & Calvi G.M. 1997. In-plane seismic response of brick masonry walls. *Earthquake Engineering and Strucural. Dynamics*, 26:1091–1112.

Montazerolghaem, M. & Jaeger, W. 2014. A comparative numerical evaluation of masonry initial shear test methods and modifications proposed for EN 1052-3. *Proc. 9th International Masonry Conference, Guimaraes, 2014.*

Popal, R. & Lissel, S.L. 2010. Numerical evaluation of existing mortar joint shear tests and a new test method. *Proc. 8th International Masonry Conference, Dresden, 2010.*

Riddington, J.R., Fong, K.H. & Jukes, P. 1997. Numerical study of failure initiation in different joint shear tests. *Masonry International*, 11(2).

Riddington, J.R. & Jukes, P. 1994. A masonry joint shear strength test method. *Proc. Instn Civ. Engrs Structs & Bldgs*, 104:267-274.

Rots, J.G. 1997. *Structural Masonry – An experimental/numerical basis for practical design rules*, Rotterdam: Balkema.

Stöckl, S., Hofmann, P. & Mainz, J. 1990. A comparative finite element evaluation of mortar joint shear tests. *Masonry International*, 3(3).

Van der Pluijm, R. 1999 Out of plane bending of masonry. *Ph.D. Thesis. Eindhoven University of Technology, The Netherlands.*

Van der Pluijm, R., Rutten, H. & Ceelen, M. 2000. Shear behaviour of bed joints. *Proc. 12th Int. Brick and Block Mas. Conf., Madrid, 25-28 June 2000.*

Van Zijl, G. 2004. Modeling masonry shear-compression: role of dilatancy highlighted. *Journal of Engineering Mechanics*, 130(11):1289-1296.

Vermeltfoort, A.T. Variation in shear properties of masonry. *Proc. 8th International Masonry Conference, Dresden, 2010.*